

## Liquid-liquid extraction process for gas separation from water in polymeric membrane: Mathematical modeling and simulation

Nahid Salimi<sup>1</sup>, Sadegh Moradi<sup>1</sup>, Afsaneh Fakhar<sup>2</sup>  
and Seyed Mohammad Reza Razavi<sup>\*2</sup>

<sup>1</sup> Department of Chemical Engineering, Faculty of Engineering, Arak University, Arak, Iran

<sup>2</sup> Young Researchers and Elite Club, South Tehran Branch, Islamic Azad University, Tehran, Iran

(Received December 12, 2015, Revised June 03, 2016, Accepted June 25, 2016)

**Abstract.** In this study, application of polypropylene hollow fiber membrane contactors for CO<sub>2</sub> removal from water in liquid-liquid extraction (LLE) mode was simulated. For this purpose, a steady state 2D mathematical model was developed. In this model axial and radial diffusion was considered to CO<sub>2</sub> permeation through the hollow fibers. CO<sub>2</sub> laden water is fed at a constant flow rate into the lumen side, permeated through the pores of membrane and at the end of this process, CO<sub>2</sub> solution in the lumen side was extracted by means of aqueous diethanolamine (DEA) and chemical reaction. The simulation results were validated with the experimental data and it was found a good agreement between them, which confirmed the reliability of the proposed model. Both simulation and experimental results confirmed the reduction in the percentage of CO<sub>2</sub> removal by increment of feed flow rate.

**Keywords:** carbon dioxide; hollow fiber; DEA; diffusion; liquid-liquid extraction; simulation

### 1. Introduction

The reasons of the presence of CO<sub>2</sub> in natural water can be atmospheric absorption of CO<sub>2</sub>, breathing of sea creatures, marine plant photosynthesis and decomposition of organic compounds in water. Although the presence of CO<sub>2</sub> in water is mostly due to natural phenomena, amount of CO<sub>2</sub> is increased significantly because of pumping industrial sewage into the water. High concentration of CO<sub>2</sub> (> 0 mg/l) in water can threat marine life (Hope *et al.* 1995, Vinci *et al.* 2004). Industrial production of solution and vapor of ammonia and urea also leads to production of sewage with high concentration of CO<sub>2</sub>. So CO<sub>2</sub> separation from water is become an important issue in recent years. Industrial and usual processes used for CO<sub>2</sub> separation are faced with some frequently reoccurring problems such as loading, channeling, foaming, flooding and also are not cost-effective (Al-Marzouqi *et al.* 2008). In recent years, researches have been focused on application of hollow fiber membrane contactors (HFMCs) which are able to degasify liquids and resolve the most of the mentioned problems and limitations. Membrane contactor has several advantages compared to common processes such as higher mass transfer rates, independent control of gas and liquid rates, known and constant interfacial area and easy scale up (Mohammadi *et al.* 2016, Miramini *et al.* 2013, IPCC 2005, Wang *et al.* 2004, Razavi *et al.* 2015a, c, Lu *et al.* 2005,

---

\*Corresponding author, Ph.D. Researcher, E-mail: [mohammadreza.razavi@ce.iut.ac.ir](mailto:mohammadreza.razavi@ce.iut.ac.ir)

Jun *et al.* 2015, Zhang *et al.* 2006, Keshavarz *et al.* 2008, Razavi and Miri 2015). Because CO<sub>2</sub> is an acid gas, chemical absorption using organic amines for CO<sub>2</sub> capture has evaluated by many authors (Lu *et al.* 2005, Sayari and Belmabkhout 2010, Hoff *et al.* 2004, Olajire 2010, Mondal *et al.* 2012). The methods that have been widely designed allow the CO<sub>2</sub> separation by absorption in alkanolamines solution in contactor (IPCC 2005, Lu *et al.* 2005, Paul *et al.* 2007). In order to gain a better understanding of CO<sub>2</sub> absorption in a HFMC, some researchers have been working on the modeling and simulation of CO<sub>2</sub> capture and studied some variables which are affective on the removal of CO<sub>2</sub>. Since using simulation of CO<sub>2</sub> removal from mixtures is more cost-effective and prevents wasting money on doing different experiments, researchers have been tending to use it for the separation studies (Zhang *et al.* 2006, Hoff *et al.* 2004, Paul *et al.* 2007). Hoff investigated the effect of CO<sub>2</sub> partial pressure, liquid CO<sub>2</sub> loading, liquid velocity and temperature on the flux of the CO<sub>2</sub> absorption rate by using aqueous solutions of monoethanolamine (MEA) and methyldiethanolamine (MDEA) as the absorbents (Hoff *et al.* 2004). A theoretical simulation was performed to study CO<sub>2</sub> capture by three typical alkanolaminesolutions of 2-amino-2-methyl-1-propanol (AMP), diethanolamine (DEA) and methyldiethanoamine (MDEA) in a HFMC. Simulation results indicated that liquid flow velocity, initial liquid concentration, the fiber length and fiber radius affect the CO<sub>2</sub> absorption significantly (Wang *et al.* 2004). In addition, Lu studied the effects of 2-Amino-2-methyl-1-propanol (AMP) and piperazine (PZ) activators on mass-transfer enhancement in a HFMC. The Activators showed effective enhancement in mass-transfer of membrane gas absorption (Lu *et al.* 2007). A two-dimensional mathematical model was developed by Al-Marzouqi for the permeation of CO<sub>2</sub> through HFMCs. That model considered axial and radial diffusion inside the fiber, through the membrane, and within the shell side of the contactor. The modeling results showed that the removal of CO<sub>2</sub> increased by enhancement of solvent concentration and liquid velocity. On the contrary, higher temperatures resulted in little effect on the rate of removal (Al-Marzouqi *et al.* 2008). It is notable that the methods involving gas-liquid contactors have operational drawbacks such as loading and flooding in the column. Therefore, liquid-liquid extraction has received more attention, recently (Agrahari *et al.* 2011). HFMC systems in LLE mode, have been used successfully in refinery systems. For example, Mansourizadeh used polyvinylidene fluoride (PVDF) hollow fiber membrane contactor for CO<sub>2</sub> stripping from water and investigated the effect of different operating conditions on the CO<sub>2</sub> stripping efficiency. In our previous studies, CO<sub>2</sub> capture from gas mixtures and natural gas in nanoporous and porous membranes was simulated (Fazaeli *et al.* 2015, Razavi *et al.* 2013, Tahvildari *et al.* 2015, Razavi *et al.* 2015a). Owing to very few studies done on removal of CO<sub>2</sub> from water under liquid-liquid extraction mode, this object was selected for this research. Since reaction of secondary amines with CO<sub>2</sub> is considerably faster than that with tertiary amines (Rinker *et al.* 1996), in this study secondary amine DEA are used as extractor liquid for CO<sub>2</sub> separation. The effect of operating conditions on the separation was studied and compared with experimental data.

## 2. Simulation

### 2.1 Model domain for simulation

In this work a two-dimensional mathematical model was developed for the CO<sub>2</sub> capture from water through hollow fiber membrane contactors (HFMCs). The separation of CO<sub>2</sub> using DEA as an absorbent in a non-aligned flow hollow fiber membrane contactor was studied. The mass

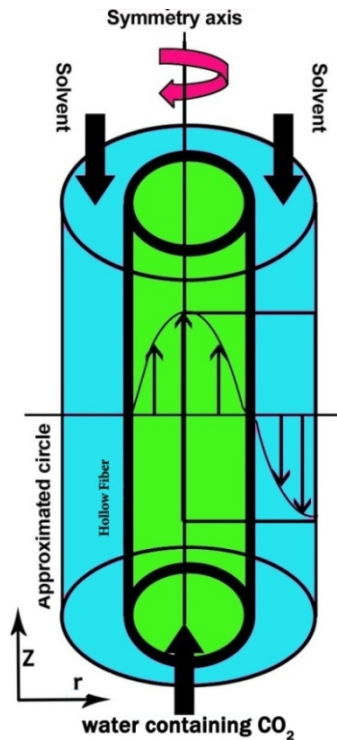


Fig. 1 The mass transfer model used for modeling (Razavi *et al.* 2016)

transfer model used for modelling is shown in Fig. 1. As shown in Fig. 1 hollow fiber is fed by water containing  $\text{CO}_2$  from a tank at constant flow rate and shell is fed by DEA at constant flow rate in a non- aligned way. The molecules of  $\text{CO}_2$  are separated from water and permeate through the pores filled with air. To keep DEA in high concentration, it is assumed  $\text{CO}_2$  molecules are reacted quickly with DEA and make no change in extracting phase resistance. Therefore,  $\text{CO}_2$  concentration is decreased exponentially from an initial level in the tank. The output water which is free of  $\text{CO}_2$  is recycled continuously and returned to the tank. The HFMC consists of three sections: lumen side, membrane and shell side. The steady state 2- dimensional model is applied for each section.

## 2.2 The characteristics of module and membrane

Hollow fibers membrane contactor was made of PP. Characteristic parameters of the membrane are given in Table 1.

## 2.3 Equations of the model

### 2.3.1 Species balance on the lumen side

The fully developed tubular flow of a liquid was assumed. The velocity profile is parabolic that allowing for diffusion in the axial and radial direction on the tube. 2D Geometry and steady state for species balance was considered, Eq. (1) under such condition can be written as follows (Bird *et al.* 1960)

Table 1 HFMC physical properties and set up operation (Criscuoli *et al.* 2003)

Parameter	Value	Reference	Parameter	Value	Reference
Inner fiber radius ( $\mu\text{m}$ )	120	-	Solvent flow rate (L/m)	1.5	-
Outer fiber radius ( $\mu\text{m}$ )	150	-	Feed flow rate (L/m)	(0.2, 0.5, 0.8)	-
$\varepsilon$ (porosity %)	40	-			-
$\tau$ (tortuosity) <sup>a</sup>	2.5	-			(Versteeg <i>et al.</i> 1998)
Number of fibers	10200	-	Henry's law constant, $m = 1/H$	$H = 2/82 \times 10^{-6} \exp(-2044/T)/(RT)$	(Versteeg <i>et al.</i> 1998)
Fiber length (cm)	25	-	$D_{\text{CO}_2\text{-lumen}}$	$1.92 \times 10^{-9}$	
Temperature (K)	298	-			

<sup>a</sup>  $\tau = 1/\varepsilon$

$$D_{\text{CO}_2\text{-tube}} \left[ \frac{\partial^2 C_{\text{CO}_2\text{-tube}}}{\partial r^2} + \frac{1}{r} \frac{\partial C_{\text{CO}_2\text{-tube}}}{\partial r} + \frac{\partial^2 C_{\text{CO}_2\text{-tube}}}{\partial z^2} \right] = V_{z\text{-tube}} \frac{\partial C_{\text{CO}_2\text{-tube}}}{\partial z} \quad (1)$$

Where  $r$  and  $z$  denote the radial and axial coordinates, respectively. In Eq. (1)  $D^{\text{CO}_2\text{-tube}}$  and  $C$  refers to diffusion coefficient of  $\text{CO}_2$  into water and the concentration of solute ( $\text{CO}_2$ ) in water at the temperature and pressure of system, respectively. The velocity profile in the lumen side under laminar flow is obtained (Bird *et al.* 1960) by

$$v_z(r) = 2\bar{V} \left[ 1 - \left( \frac{r}{r_1} \right)^2 \right] \quad (2)$$

Where  $\bar{V}$  is the average velocity in the lumen,  $r$  is the radial distance,  $v_z$  is the velocity of stream at  $r$  and  $r_1$  is the inner radius of the lumen. The average velocity in the lumen can be defined as

$$\bar{V} = \frac{Q}{N\pi r_1^2} \quad (3)$$

Where  $Q$  is flow rate of feed and  $N$  is number of fibers.

Boundary conditions considered for the lumen side are as follows

$$\text{at } z = 0 \quad c_{\text{CO}_2\text{-Lumen}} = c_{o,\text{CO}_2} \quad (4)$$

$$\text{at } z = L \quad \text{Convective Flux} \quad (5)$$

$$\text{at } r = r_1 \quad c_{\text{CO}_2\text{-lumen}} = c_{\text{CO}_2\text{-membrane}} \quad (6)$$

$$\text{at } r = 0 \quad \frac{\partial c_{co2-Lumen}}{\partial r} = 0 \quad (\text{symmetry}) \quad (7)$$

### 2.3.2 Membrane equations

CO<sub>2</sub> transmission into the membrane pores is just conducted by diffusion mechanism. The continuity equation will be simplified by steady state and no reaction assumptions as follows (Bird *et al.* 1960)

$$D_{CO_2-membrane} \left[ \frac{\partial^2 C_{CO_2-membrane}}{\partial r^2} + \frac{1}{r} \frac{\partial C_{CO_2-membrane}}{\partial r} + \frac{\partial^2 C_{CO_2-membrane}}{\partial z^2} \right] = 0 \quad (8)$$

In which boundary conditions can be written as follows

$$\text{at } r = r_1 \quad c_{co2-membrane} = c_{co2-Lumen} \quad (9)$$

$$\text{at } r = r_2 \quad c_{co2-membrane} = c_{co2-shell / m} \quad (\text{base on Henry's law}) \quad (10)$$

$$\text{at } z = 0 \quad \frac{\partial c_{co2-membrane}}{\partial r} = 0 \quad (\text{isolation}) \quad (11)$$

$$\text{at } z = 0 \quad \frac{\partial c_{co2-membrane}}{\partial r} = 0 \quad (\text{isolation}) \quad (12)$$

### 2.3.3 Shell side equations

The steady-state continuity equation in the shell side is expressed as below (Bird *et al.* 1960)

$$D_{CO_2-Shell} \left[ \frac{\partial^2 C_{CO_2-Shell}}{\partial r^2} + \frac{1}{r} \frac{\partial C_{CO_2-Shell}}{\partial r} + \frac{\partial^2 C_{CO_2-Shell}}{\partial z^2} \right] = V_{z-Shell} \frac{\partial C_{CO_2-Shell}}{\partial z} - R_{CO_2} \quad (13)$$

As stated before, by solving Navier-Stokes equation, velocity distribution in the shell side can be obtained by (Bird *et al.* 1960)

$$\begin{aligned} -\nabla \cdot \eta \left( \nabla V_{z-Shell} + (\nabla V_{z-Shell})^T \right) + \rho (V_{z-Shell} \cdot \nabla) V_{z-Shell} + \nabla p = F \\ \nabla V_{z-Shell} = 0 \end{aligned} \quad (14)$$

$V$  (m/s),  $P$  (Pa),  $\rho$  (kg m<sup>-3</sup>),  $\eta$  (kg m<sup>-1</sup> s<sup>-1</sup>) and  $F$  (N) denote velocity, pressure, density, dynamic viscosity and body force, respectively. The shell radius can be estimate by applying Happel free surface model (Happel 1959)

$$r_3 = \left( \frac{1}{1-\phi} \right)^{1/2} r_2 \quad (15)$$

Where  $r_2$  indicate the tube outer radius.  $\Phi$  is volume fraction of void section and can be defined by

$$1 - \phi = \frac{nr^2}{R^2} \quad (16)$$

Where  $n$  and  $R^2$  are the number of fibers and inner radius of modules, respectively. Boundary conditions used for the shell are as follows

$$\text{at } r = r_2 \quad c_{co2-shell} = c_{co2-membrane} * m \quad (17)$$

$$\text{(isolation) at } r = r_3 \quad \frac{\partial c_{co2-shell}}{\partial r} = 0 \quad (18)$$

$$\text{at } z = L \quad c_{co2-shell} = 0 \quad (19)$$

$$\text{at } z = 0 \quad \text{Convective Flux} \quad (20)$$

#### 2.3.4 DEA equations in shell side

The steady state continuity equation for DEA absorber is written as follows

$$D_{i-shell} \left[ \frac{\partial^2 C_{i-shell}}{\partial r^2} + \frac{1}{r} \frac{\partial C_{i-shell}}{\partial r} + \frac{\partial^2 C_{i-shell}}{\partial z^2} \right] = V_{z-shell} \frac{\partial C_{i-shell}}{\partial z} - R_i \quad (21)$$

$R_i$  denotes the chemical reaction between CO<sub>2</sub> and DEA absorber. Boundary conditions required for solving Eq. (21) is given as follows

$$\text{at } z = L \quad c_{DEA-shell} = c_{M0} \quad (22)$$

$$\text{at } z = 0 \quad \text{Convective Flux} \quad (23)$$

$$\text{at } r = r_2 \quad \frac{\partial c_{DEA-shell}}{\partial r} = 0 \quad \text{(isolation)} \quad (24)$$

$$\text{at } r = r_3 \quad \frac{\partial c_{DEA-shell}}{\partial r} = 0 \quad \text{(symmetry)} \quad (25)$$

## 4. Numerical solution

The equations related to the lumen side, the membrane, the shell side, with the appropriated boundary conditions were solved using COMSOL Multiphysics version 4.2 software, which uses finite element method for numerical solutions of the model equations. The finite element analysis

is combined with adaptive meshing and error using numerical solver of UMFPACK version. The applicability and accuracy of UMFPACK for solving membrane equations have been asserted by some researchers (Ghadiri *et al.* 2013a, b, Bishnoi and Rochelle 2000, Shirazian *et al.* 2009, Tahvildari *et al.* 2015, Fadaei *et al.* 2011).

## 5. Result and discussion

### 5.1 Model validation

Simulation results for CO<sub>2</sub> removal from water has been compared with experimental data based on Table 2. This comparison was done by using experimental data of Agrahari's research (Agrahari *et al.* 2011) for 300 ppm CO<sub>2</sub> concentration contained feed. The percent removal of CO<sub>2</sub> decreases with increasing feed flow rate. The maximum removal (approximately 95%) obtained at the lowest feed flow rate (0.2 L/min) (The removal decreases to approximately 90% at 0.8 L/min) (Agrahari *et al.* 2011). Furthermore, according to Table 2 good correlation is seen between

Table 2 Comparison between the percent removal of CO<sub>2</sub> by simulation and experimental study (Agrahari *et al.* 2011)

Solvent flow rate (L/min)	Feed flow rate (L/min)	Experimental (CO <sub>2</sub> %)	Simulation (CO <sub>2</sub> %)
1.5	0.2	0.95	0.92
1.5	0.5	0.92	0.88
1.5	0.8	0.9	0.87

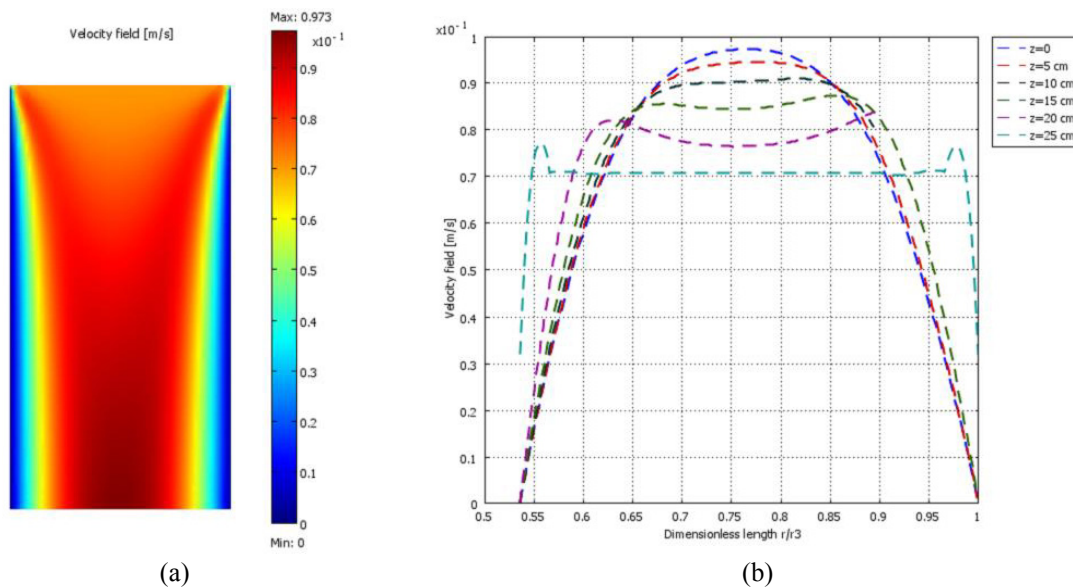


Fig. 2 (a) Velocity field in the shell side of HFMC; (b) Velocity profiles in the shell side along the membrane different length. Feed flow rate = 0.5 L/min; solvent(DEA) flow rate = 1.5 L/min; CO<sub>2</sub> inlet concentration =  $6 \times 10^{-3}$  mol/L; DEA inlet concentration = 1 mol/L; T = 298 K

simulation and experimental results of percent removal of CO<sub>2</sub> and there is a same trend in variation of CO<sub>2</sub> capture by changing feed flow rate in both studies. This agreement ensures the efficiency of this model for larger scales.

### 5.2 Velocity distribution

The velocity field and its profile in the shell side of hollow fiber membrane, where the absorbent flows, are shown in Figs. 2(a) and (b). The velocity profile in the shell side was simulated by solving the Navier-Stokes equations. The velocity profile is almost parabolic and the maximum velocity is appeared at the center of the shell. Moreover, velocity is zero on the two shell walls due to assumed no-slip conditions. Figs. 2(a) and (b) also display that velocity profile becomes fully developed after a short distance from the entrance of the shell side.

### 5.3 Concentration distribution of CO<sub>2</sub> in the HFMC

The dimensionless concentration of CO<sub>2</sub> ( $c/c_0$ ) in the lumen side, the membrane and the shell side of the HFMC are shown in Fig. 3. The feed containing CO<sub>2</sub> flows from one side of the HFMC ( $z = 0$ ) where the concentration of CO<sub>2</sub> is the maximum. Liquid solvent (DEA) flows from the other side ( $z = L$ ) where the concentration of feed is assumed to be zero. As the CO<sub>2</sub> flows through the lumen side, it is transferred towards the membrane due to concentration difference (driving force) (Shirazian *et al.* 2009). The mechanisms of mass transfer in the lumen and shell sides are convection and diffusion. The mechanism of convection in the  $z$ -direction is axial, while the mechanism of diffusion in the  $r$ - direction is radial. Gas mixture is transferred to the other side through the membrane pores and the mobile solvent in the shell side can absorb the CO<sub>2</sub>.

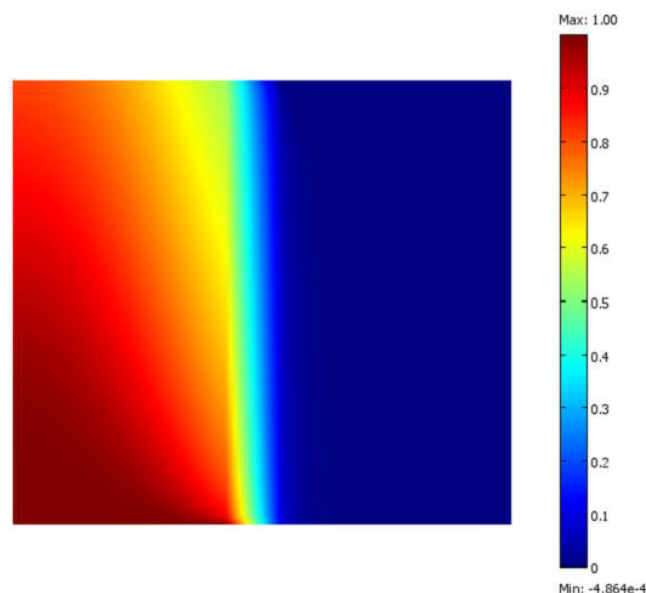


Fig. 3 Concentration distribution of CO<sub>2</sub> in the HFMC, feed flow rate = 0.5 L/min; solvent flow rate = 1.5 L/min; CO<sub>2</sub> inlet concentration =  $6 \times 10^{-3}$  mol/L; DEA inlet concentration = 1 mol/L;  $T = 298$  K



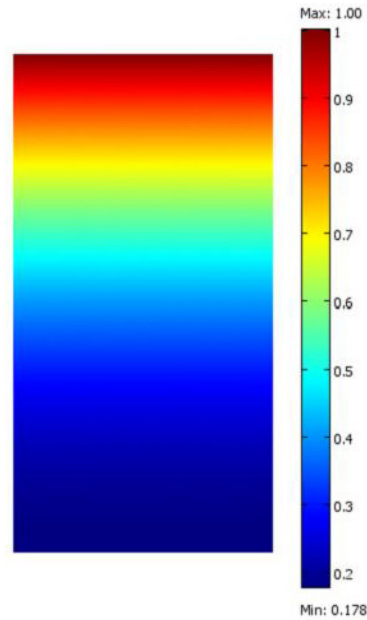


Fig. 4 Dimensionless concentration distribution of DEA in the shell side of the HFMC, feed flow rate = 0.5 L/min; solvent flow rate = 1.5 L/min; CO<sub>2</sub> inlet concentration =  $6 \times 10^{-3}$  mol/L; DEA inlet concentration = 1 mol/L;  $T = 298$  K

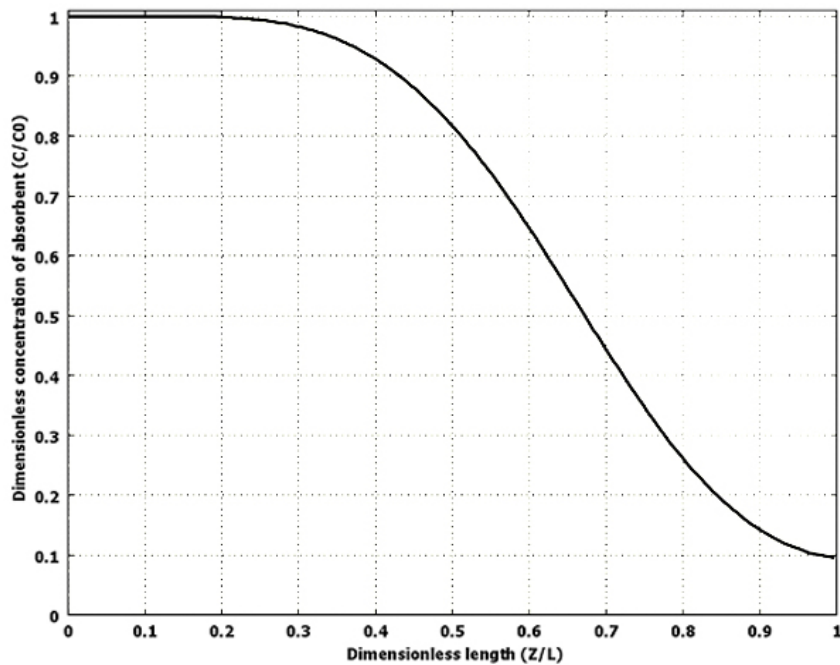


Fig. 5 Axial concentration distribution of DEA along the HFMC, feed flow rate = 0.5 L/min; solvent flow rate = 1.5 L/min; CO<sub>2</sub> inlet concentration =  $6 \times 10^{-3}$  mol/L; DEA inlet concentration = 1 mol/L;  $T = 298$  K

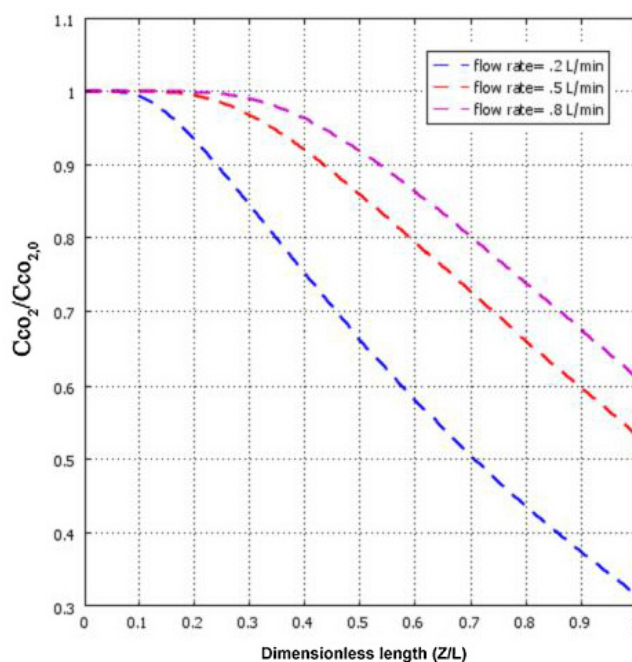


Fig. 6 Dimensionless  $\text{CO}_2$  outlet concentration profile of at the different flow rate of feed; solvent flow rate = 1.5 L/min;  $\text{CO}_2$  inlet concentration =  $6 \times 10^{-3}$  mol/L; DEA inlet concentration = 1 mol/L;  $T = 298$  K

#### 5.4 Concentration distribution of DEA in the HFMC

Fig. 4 represents dimensionless concentration distribution of amine (DEA) in the shell side of the HFMC. The amine solution flows through the shell side and reacts with  $\text{CO}_2$  which come from the membrane pores due to the concentration difference between the two sides of the membrane. The amine concentration decrease significantly in the interface zone. Fig. 5 indicates axial concentration distribution of DEA along the contactor. Since  $\text{CO}_2$  concentration in the entrance of shell side is negligible, the absorber concentration is reduced in the middle of HFMC length faster than the entrance region of HFMC.

#### 5.5 Effects of feed flow rate on $\text{CO}_2$ outlet concentration

Fig. 6 displays dimensionless concentration of  $\text{CO}_2$  along the tube side at different flow rates of feed stream. Enhancement of feed flow rate results in reduction of feed residence time in the tube and as a result absorption rate of carbon dioxide declines.  $C_{\text{outlet}}$  ( $\text{mol}/\text{m}^3$ ) is calculated by integrating the local concentration at the outlet of the lumen side ( $z = L$ )

$$C_{\text{outlet}} = \frac{\int_{r=0}^{r=r_1} \int c(r) dA}{\int_{r=0}^{r=r_1} \int dA} \Bigg|_{z=L} \quad (26)$$

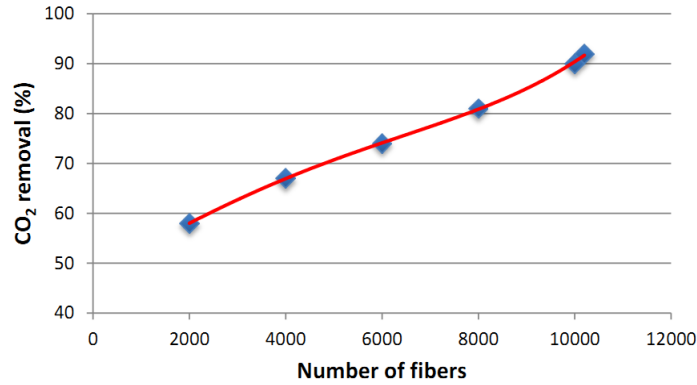


Fig. 7 Effect of fiber number on CO<sub>2</sub> removal(%). solvent flow rate = 1.5 L/min; CO<sub>2</sub> inlet concentration =  $6 \times 10^{-3}$  mol/L; DEA inlet concentration = 1 mol/L;  $T = 298$  K

Based on Fig. 6, CO<sub>2</sub> concentration drops suddenly due to high reaction with the solvent (DEA) and by reduction of feed flow rate, decline in dimensionless concentration is enhanced.

### 5.6 Effect of Number of Fibers on the Removal of CO<sub>2</sub>

Number of fibers as an important factor on performance of membrane contactors has been shown in Fig. 7. In this Figure, CO<sub>2</sub> removal on outlet increases by grows in number of fibers. As in number of 10200, maximum amount of CO<sub>2</sub> removal has been obtained. This is due to increase of mass transfer area between CO<sub>2</sub> and DEA, by increase in number of fiber.

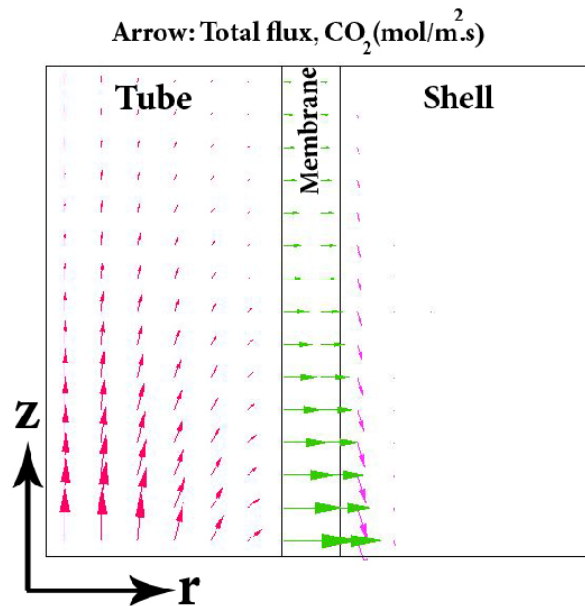


Fig. 8 Vector of total flux for CO<sub>2</sub> in the membrane contactor. solvent flow rate = 1.5 L/min; CO<sub>2</sub> inlet concentration =  $6 \times 10^{-3}$  mol/L; DEA inlet concentration = 1 mol/L;  $T = 298$  K

### 5.7 Total flux for CO<sub>2</sub> in the three section of membrane contactor

Fig. 8 mention the vector of carbon dioxide concentration in the membrane contactor. It is clearly illustrated that CO<sub>2</sub> mass transfer flux reduces along the membrane module that due to carbon dioxide removal by DEA. Moreover, variation rate of CO<sub>2</sub> concentration along the contactor is significant which confirms the capability of membrane contactor as a good process for CO<sub>2</sub> capture.

## 4. Conclusions

In this study chemical absorption of CO<sub>2</sub> in amine solution DEA in hollow fiber membrane contactor was investigated. A 2-dimensional geometry was used to describe CO<sub>2</sub> removal process. Simulation results showed that CO<sub>2</sub> removal was completely done by DEA, and the results were validated with the experimental data. The modeling showed a good agreement between simulation and experimental results. The effect of feed flow rate on CO<sub>2</sub> removal from water was also studied. Absorption rate of carbon dioxide declined by increase of feed flow rate, enhancement of feed flow rate results in reduction of feed residence time in the tube and as a result absorption rate of carbon dioxide declines. This agreement ensures the efficiency of this model for larger scales.

## References

- Agrahari, G.K., Verma, N. and Bhattacharya, P.K. (2011), "Application of hollow fiber membrane contactor for the removal of carbon dioxide from water under liquid-liquid extraction mode", *J. Membr. Sci.*, **375**(1-2), 323-333.
- Al-Marzouqi, M.H., El-Naas, M.H., Marzouk, S.A.M., Al-Zarooni, M.A., Abdullatif, N. and Faiz, R. (2008), "Modeling of CO<sub>2</sub> absorption in membrane contactors", *Sep. Purif. Technol.*, **59**(3), 286-293.
- Bird, R.B., Stewart, W.E. and Lightfoot, E.N. (1960), *Transport Phenomena*, (2nd Ed.), John Wiley & Sons, New York, NY, USA.
- Bishnoi, S. and Rochelle, G.T. (2000), "Absorption of carbon dioxide into aqueous piperazine: reaction kinetics, mass transfer and solubility", *Chem. Eng. Sci.*, **55**(22), 5531-5543.
- Bothun, G.D., Knutson, B.L., Strobel, H.J., Nokes, S.E., Brignole, E.A. and Díaz, S. (2003), "Compressed solvents for the extraction of fermentation products within a hollow fiber membrane contactor", *J. Supercrit. Fluid.*, **25**(2), 119-134.
- Criscuoli, A., Drioli, E. and Moretti, U. (2003), "Membrane contactors in the beverage industry for controlling the water gas composition", *Ann. N.Y. Acad. Sci.*, **984**, 1-16.
- Fadaei, F., Shirazian, S. and Ashrafizadeh, S.N. (2011), "Mass transfer simulation of solvent extraction in hollow-fiber membrane contactors", *Desalination*, **275**(1-3), 126-132.
- Fazaeli, R., Razavi, S.M.R., Najafabadi, M.S. and Torkaman, R. (2015), "Computational simulation of CO<sub>2</sub> removal from gas mixtures by chemical absorbents in porous membranes", *RSC Advances*, **5**(46), 36787-36797.
- Ghadiri, M., Fakhri, S. and Shirazian, S. (2013), "Modeling and CFD simulation of water desalination using nanoporous membrane contactors", *Ind. Eng. Chem. Res.*, **52**(9), 3490-3498.
- Ghadiri, M., Ghasemi Darehnaei, M., Sabbaghian, S. and Shirazian, S. (2013), "Computational simulation for transport of priority organic pollutants through nanoporous membranes", *Chem. Eng. Technol.*, **36**(3), 507-512.
- Happel, J. (1959), "Viscous flow relative to arrays of cylinders", *AIChE J.*, **5**(2), 174-177.
- Hoff, K.A., Juliussen, O., Falk-Pedersen, O. and Svendsen, H.F. (2004), "Modeling and experimental study

- of carbon dioxide absorption in aqueous alkanolamine solutions using a membrane contactor”, *Ind. Eng. Chem. Res.*, **43**(16), 4908-4921.
- Hope, D., Dawson, J.J.C., Cresser, M.S. and Billett, M.F. (1995), “A method for measuring free CO<sub>2</sub> in upland streamwater using headspace analysis”, *J. Hydrol.*, **166**(1-2), 1-14.
- IPCC (2005), IPCC Special Report on Carbon Dioxide Capture and Storage; Cambridge University Press, United Nations, New York, NY, USA.
- Jun, C.L., Xiang, J.Y. and Dong, H.Y. (2015), “CFD simulations of the fluid flow behavior in a spacer-filled membrane module”, *Membr. Water Treat., Int. J.*, **6**(6), 513-524.
- Keshavarz, P., Fathikalajahi, J. and Ayatollahi, S. (2008), “Analysis of CO<sub>2</sub> separation and simulation of a partially wetted hollow fiber membrane contactor”, *J. Hazard. Mater.*, **152**(3), 1237-1247.
- Lu, J., Wang, L., Sun, X., Li, J. and Liu, X. (2005), “Absorption of CO<sub>2</sub> into aqueous solutions of methyldiethanolamine and activated methyldiethanolamine from a gas mixture in a hollow fiber contactor”, *Ind. Eng. Chem. Res.*, **44**(24), 9230-9238.
- Lu, J.G., Zheng, Y.F., Cheng, M.D. and Wang, L.J. (2007), “Effects of activators on mass-transfer enhancement in a hollow fiber contactor using activated alkanolamine solutions”, *J. Membr. Sci.*, **289**(1-2), 138-149.
- Miramini, S.A., Razavi, S.M.R., Ghadiri, M., Mahdavi, S. and Moradi, S. (2013), “CFD simulation of acetone separation from an aqueous solution using supercritical fluid in a hollow-fiber membrane contactor”, *Chem. Eng. Process.: Process Intensification*, **72**, 130-136.
- Mohammadi, M., Marjani, A., Asadollahzadeh, M., Hemmati, A. and Kazemi, S.M. (2016), “Simulation of transport phenomena in porous membrane evaporators using computational fluid dynamics”, *Membr. Water Treat., Int. J.*, **7**(2), 87-100.
- Mondal, M.K., Balsora, H.K. and Varshney, P. (2012), “Progress and trends in CO<sub>2</sub> capture/separation technologies: A review”, *Energy*, **46**(1), 431-441.
- Olajire, A.A. (2010), “CO<sub>2</sub> capture and separation technologies for end-of-pipe applications – A review”, *Energy*, **35**(6), 2610-2628.
- Paul, S., Ghoshal, A.K. and Mandal, B. (2007), “Removal of CO<sub>2</sub> by single and blended aqueous alkanolamine solvents in hollow-fiber membrane contactor: Modeling and simulation”, *Ind. Eng. Chem. Res.*, **46**(8), 2576-2588.
- Razavi, S.M.R. and Miri, T. (2015), “A real petroleum refinery wastewater treatment using hollow fiber membrane bioreactor (HF-MBR)”, *J. Water Process Eng.*, **8**, 136-141.  
DOI: <http://dx.doi.org/10.1016/j.jwpe.2015.09.011>
- Razavi, S.M.R., Razavi, S.M.J., Miri, T. and Shirazian, S. (2013), “CFD simulation of CO<sub>2</sub> capture from gas mixtures in nanoporous membranes by solution of 2-amino-2- methyl-1-propanol and piperazine”, *Int. J. Greenh. Gas Con.*, **15**, 142-149.
- Razavi, S.M.R., Shirazian, S. and Najafabadi, M.S. (2015a), “Investigations on the ability of di-isopropanol amine solution for removal of CO<sub>2</sub> from natural gas in porous polymeric membranes”, *Polym. Eng. Sci.*, **55**(3), 598-603.
- Razavi, S.M.R., Marjani, A. and Shirazian, S. (2015b), “CO<sub>2</sub> capture from gas mixtures by alkanol amine solutions in porous membranes”, *Transp. Porous. Med.*, **106**(2), 323-338.
- Razavi, S.M.R., Miri, T., Barati, A., Nazemian, M. and Sepasi, M. (2015c), “Industrial wastewater treatment by using of membrane”, *Membr. Water Treat., Int. J.*, **6**(6), 489-499.
- Razavi, S.M.R., Shirazian, S. and Nazemian, M. (2016), “Numerical simulation of CO<sub>2</sub> separation from gas mixtures in membrane modules: Effect of chemical absorbent”, *Arab. J. Chem.*, **9**(1), 62-71.
- Rinker, E.B., Ashour, S.S. and Sandall, O.C. (1996), “Kinetics and modeling of carbon dioxide absorption into aqueous solutions of diethanolamine”, *Ind. Eng. Chem. Res.*, **35**(4), 1107-1114.
- Sayari, A. and Belmabkhout, Y. (2010), “Stabilization of amine-containing CO<sub>2</sub> adsorbents: Dramatic effect of water vapor”, *J. Am. Chem. Soc.*, **132**(18), 6312-6314.
- Shirazian, S., Moghadassi, A. and Moradi, S. (2009), “Numerical simulation of mass transfer in gas-liquid hollow fiber membrane contactors for laminar flow conditions”, *Simul. Model. Practice Theory*, **17**(4), 708-718.

- Tahvildari, K., Razavi, S.M.R., Tavakoli, H., Mashayekhi, A. and Golmohammadzadeh, R. (2015), "Modeling and simulation of membrane separation process using computational fluid dynamics", *Arab. J. Chem.*, **9**(1), 72-78.
- Versteeg, G.F. and Van Swaaij, W.P.M. (1988), "On the kinetics between CO<sub>2</sub> and alkanolamines both in aqueous and non-aqueous solutions. I. Primary and secondary amines", *Chem. Eng. Sci.*, **43**(3), 573-585.
- Vinci, B.J., Summerfelt, S.T., Creaser, D.A. and Gillette, K. (2004), "Design of partial water reuse systems at White River NFH for the production of Atlantic salmon smolt for restoration stocking", *Aquacult. Eng.* **32**(1), 225-243.
- Wang, R., Li, D.F. and Liang, D.T. (2004), "Modeling of CO<sub>2</sub> capture by three typical amine solutions in hollow fiber membrane contactors", *Chem. Eng. Process.*, **43**(7), 849-856.
- Zhang, H.Y., Wang, R., Liang, D.T. and Tay, J.H. (2006), "Modeling and experimental study of CO<sub>2</sub> absorption in a hollow fiber membrane contactor", *J. Membr. Sci.*, **279**(1-2), 301-310.

CC